

# Distributed Effects Model for Cascaded Traveling-Wave Electroabsorption Modulator

Yi-Jen Chiu, *Member, IEEE*, Volkan Kaman, *Member, IEEE*, Sheng Z. Zhang, *Member, IEEE*, and John E. Bowers, *Fellow, IEEE*

**Abstract**—A distributed model based on the large-signal electrooptic conversion is proposed to analyze cascaded traveling-wave electroabsorption modulators (TWEAMs) for high-speed optical switching applications. The microwave propagation loss, velocity mismatch, as well as frequency chirping are included. The model predicts that a cascaded TWEAM structure has the advantage of a high design tolerance to various distributed effects and an improved extinction ratio and optical loss in comparison to a single device of same total length. The agreement between experimental and calculated results indicates that the cascaded structures can be implemented for efficient TWEAM design.

**Index Terms**—Cascaded structures, distributed, electroabsorption, optical fiber communication, tandem, traveling-wave devices.

## I. INTRODUCTION

THERE is a lot of recent interest in optical time division multiplexed (OTDM) systems based on high-speed optical switching of electroabsorption modulators (EAM) [1]–[3]. For four-channel OTDM systems beyond 100 Gb/s, the optical pulses require short pulsewidths (<3 ps) and high dynamic extinction ratios (>30 dB) to reduce interchannel interference, as well as high average optical output powers (> -25 dBm) to ensure sufficient system signal-to-noise ratios (SNR). Therefore, a high ON-OFF ratio with high-speed low-loss low-chirp operation is necessary for EAM-based optical short pulse sources. Recently, traveling-wave EAMs (TWEAM) have been demonstrated to overcome the *RC*-lump bandwidth limitation with low-drive voltage requirements and high extinction ratios [4]. Furthermore, tandem EAMs achieve higher dynamic extinction ratios with reduced optical pulsewidths [5], [6], but the design or optimization of devices are not considered. The impact of distributed effects on TWEAMs has previously been analyzed in the linear electrooptical conversion regime (small signal model) [7]. However, to obtain the short switching window, the intrinsic nonlinear absorption of EAMs need to be considered as well. Therefore, it is imperative to analyze the design and the optimization of EAMs for optical switching applications. In this letter, we propose a distributed model based on the nonlinear

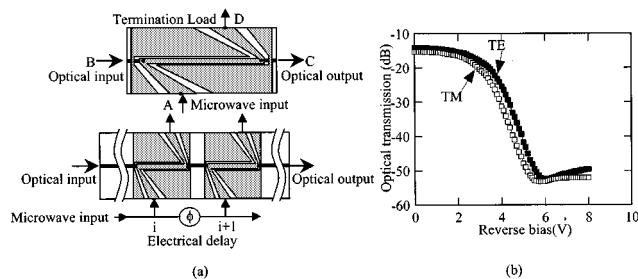


Fig. 1. (a) (top) The schematic diagram of single TWEAM. AB, CD are the CPW lines, BC is p-i-n waveguide. (bottom) The schematic diagram (*i*)th and (*i* + 1)th section of cascade TWEAMs, and between adjacent sections the delay  $\phi$  is for the phase matching. (b) The normalized measured TE (solid square) and TM (open square) optical transmission with bias [5] for 400- $\mu$ m-long TWEAM [5]. In this letter, the calculation is based on the TM-mode.

electrooptic-conversion effects (large signal model). Theoretically, single and cascaded TWEAMs of the same length are calculated to compare the performance. The model is verified by the experiment results [5]. In the view points of design, the cascaded TWEAM structures have the advantages over the single one in the application of optical switching.

## II. THE DISTRIBUTED MODEL

A split-step method [8] is used to calculate the optical pulse evolution in the waveguide. The schematic diagram of the single and cascaded TWEAM structures analyzed is shown in Fig. 1(a). The optical input power is absorbed as the microwave signal propagates along the waveguide. The time-dependent optical output intensity  $P(t)$  can be expressed by

$$P(t) = A \cdot \left[ \exp \left( -\alpha_o L - \int_0^L \Delta \bar{k} \left( z, t' + t - \frac{L}{v_o} \right) \cdot dz \right) \right]$$

$$\Delta \bar{k}(z, t) = \Delta \alpha(z, t) + j \cdot \Delta n(z, t) \cdot k_o$$

$$z = v_o \cdot t' \quad j = \sqrt{-1} \quad k_o = 2\pi/\lambda_o \quad (1)$$

where

the factor  $A$  includes the optical input power intensity and the fiber coupling losses at both ends;  
 $v_o$  optical group velocity;  
 $\alpha_o$  optical loss at zero bias;  
 $L$  waveguide length;  
 $\lambda_o$  optical wavelength;

Manuscript received November 10, 2000; revised April 10, 2001.

Y.-J. Chiu, V. Kaman, and J. E. Bowers are with the Department of Electrical and Computer Engineering, University of California, Santa Barbara, Santa Barbara, CA 93106 USA (e-mail: chiu@opto.ucsb.edu).

S. Z. Zhang was with the Department of Electrical and Computer Engineering, University of California, Santa Barbara, Santa Barbara, CA 93106 USA. He is now with Zaffire, Inc., San Jose, CA 95134 USA.

Publisher Item Identifier S 1041-1135(01)06431-X.

$t'$  time for the optical wave to travel from the input to position  $z$ .

The voltage-dependent optical wave number relative to zero bias  $\Delta\bar{k}(z, t)$  comprises of the real part  $\Delta\alpha(z, t)$ , which is the modal absorption coefficient change due to the electroabsorption effect, and the imaginary part  $\Delta n(z, t) \cdot k_0$ , which is the phase change due to chirping effects in modulator.  $\Delta\alpha(z, t)$  and  $\Delta n(z, t) \cdot k_0$  can be empirically extracted by dc optical transmission and optical fiber transmission [11]. Equation (1) expresses the distributed electroabsorption effects along the waveguide; at position  $z$ , optical absorption takes place only with the simultaneously applied voltage. Therefore, if the time-dependent voltage evolution along the waveguide is known, the optical pulse characteristics, including pulsewidth, optical power, extinction ratio, and phase changes can be obtained. The model also incorporates the effects of microwave propagation and velocity mismatch between the optical and electrical fields on the generated optical pulses. The distributed voltage along the waveguide can be expressed as  $V(z, t) = V_{dc} + V_{ac}(z, t)$ , where  $V_{dc}$  is the applied reverse bias, and  $V_{ac}(z, t)$  is the microwave signal. Assuming low optical power excitation in the waveguide (no optical power saturation [9] and low photocurrent on voltage-control absorption [7]), the microwave characteristics of the TWEAM are calculated by using an equivalent circuit model, and then are verified by  $s$ -matrix measurement [9]. The microwave propagation calculation is based on a linear two-port transmission matrix in frequency domain [10].

### III. CALCULATED RESULTS

The model described in the preceding section was employed to investigate and compare the distributed effects on a single TWEAM device, as well as cascaded devices. An optical group index of 3.2 was assumed, while the microwave index was varied from 3.2 (velocity-matched case) to 10. Also, microwave propagation losses were incorporated by varying the field attenuation from 0 (lossless case) to  $10 \text{ cm}^{-1}$  [4]. The  $400\text{-}\mu\text{m}$  device absorption characteristics of the TWEAM were extracted from experimental results [see Fig. 1(b)] [5]. The  $40\text{-GHz}$  sinusoidal microwave modulation input was  $7V_{pp}$  at a reverse bias of  $-4 \text{ V}$ .

The simulated optical pulsewidths, average optical output powers, and extinction ratios for a single TWEAM as a function of device length are shown in Fig. 2. For the velocity-mismatch cases without microwave propagation loss, it is observed that the pulsewidth decreases monotonically with device length due to the walkoff effect [see Fig. 2(a)]. However, pulse shortening with longer devices is at the expense of deteriorated average optical output power and extinction ratio during propagation [see Fig. 2(b)]. Additionally, when the walkoff time between the optical and electrical pulses reaches the half cycle of the electrical repetition rate for high velocity mismatch, given by  $(L/v_o - L/v_e) \approx 1/(2 \cdot f)$ , the optical pulses start broadening. On the other hand, comparing the cases with a fixed velocity mismatch and varied microwave propagation losses, the pulsewidths exhibit a slight dependence on device length [see Fig. 2(a)]; however, the average output power and

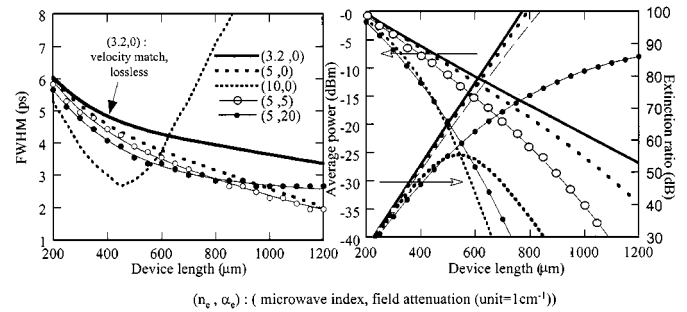


Fig. 2. (a) The generated optical pulsewidth is full-width at half-maximum of single TWEAM as function of device length at different microwave characteristics. (b) The output average power and extinction ratio of single TWEAM as function of device length at different microwave characteristics. The optical power is normalized. The dash curves are the effects including the microwave loss without changing the index.

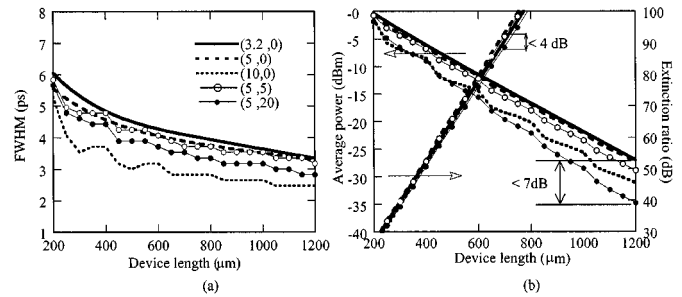


Fig. 3. (a) The cascaded TWEAM (each section is  $200 \mu\text{m}$  long) optical pulsewidth with total device length. (b) The cascaded TWEAM output average power and extinction ratio with total device length. The output power is normalized. The variation at different microwave characteristics is less than 4 dB and 7 dB for power and extinction ratio respectively.

extinction ratio deteriorate as the microwave loss increases. For a  $600\text{-}\mu\text{m}$ -long TWEAM with a microwave loss increase from 5 to  $20 \text{ cm}^{-1}$ , the optical output power and extinction ratio are both decreased by 10 dB, while the pulsewidth is shortened only by 0.1 ps. From these calculations, it can be concluded that for a single TWEAM affected by velocity mismatch and microwave propagation loss, only a slight pulse shortening will be achieved for longer devices, which are of limited use due to the degradation in optical output power and extinction ratio.

The negative impacts of walkoff, between the optical and electrical pulses, can be eliminated by phase adjustment in a cascaded TWEAM structure. The cascaded structure also compensates for the microwave losses by resupplying microwave RF power at each TWEAM. For comparative purposes, the total length of the cascade was chosen to match the single device length calculations. Since  $200\text{-}\mu\text{m}$ -long TWEAMs have negligible distributed effects (Fig. 2), each of the cascaded devices were chosen to be  $200 \mu\text{m}$  long with the last device length varied within  $200 \mu\text{m}$ . Adjusting the input microwave phases at each section for maximum optical output power ensured velocity matching throughout the cascade. Practically, the phase adjustment can be implemented by the different CPW lines [see Fig. 1(a)]. For the same velocity mismatch and microwave loss conditions as used in the single TWEAM calculations, the optical pulsewidths in the cascade configuration show small variations with a close agreement to the ideal case of no velocity mismatch or microwave loss [see Fig. 3(a)]. Furthermore, the

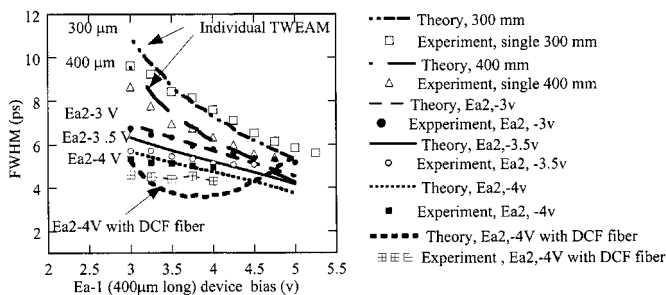


Fig. 4. The pulsewidth with device bias. The dot- and line-curves are the experiment and calculated results. The top two curves are the individual TWEAMs in the tandem structure [5] (Ea-1: 400  $\mu\text{m}$ , Ea-2: 300  $\mu\text{m}$ ). The bottom four curves are the tandem TWEAM response (from top, the Ea-2 bias: 3, 3.5, and 4 v, the lowest curve: Ea-2 bias 4 V). The lowest curve is the pulsewidth after DCF fiber transmission.

optical output power and the extinction ratio for the cascaded TWEAMs, also exhibit very little degradation despite the varied design parameters [see Fig. 3(b)]. For cascaded device lengths less than 1000  $\mu\text{m}$ , the variation in optical output power and extinction ratio are within 7 dBm and 4 dB, respectively, for various velocity mismatch and microwave propagation loss cases. These results indicate that a high tolerance to distributed effects can be obtained in the design of cascaded TWEAMs in comparison to a single device for optical short-pulse applications.

To further verify the validity of the distributed model, it was used to fit the experimental 30-GHz optical short pulse generation results in [5], where 300- and 400- $\mu\text{m}$  long tandem integrated TWEAMs were employed. The experimental static optical transmission measurements [see Fig. 1(b)] were used to extract the optical absorption change  $\Delta\alpha(V)$  for an applied voltage [5], while all the parameters of the optical ridge waveguide and microwave coplanar waveguide lines were adjusted to fit the scattering matrix (*s*-parameters). The chirp parameter was estimated to be from  $-0.4$  to  $-0.8$  for reverse biases, and from  $-3$  to  $-5$  V chirp measurement.

As in the experiment, a  $7V_{pp}$  30-GHz sinusoidal modulation was applied to both devices for optical short pulse generation. The experimental and calculated pulsewidths as a function of reverse bias for the individual devices (the other device is off), and the tandem operation is shown in Fig. 4. In order to check the chirping effect, the lowest curve of Fig. 4 is the pulsewidth after transmitting on dispersion-compensation fiber (DCF),  $-6$  ps/nm at 1540 nm. The calculated results based on the distributed model are in excellent agreement with the experimental results, which verifies the fact that the distributed model

can be used to optimize the design of high-bandwidth low-drive TWEAM structures for high-speed optical switching applications in OTDM systems.

#### IV. SUMMARY

We have developed a distributed model for accurately calculating high-speed optical short pulse generation characteristics of TWEAMs. The model includes distributed effects of microwave propagation loss and velocity mismatch between the electrical and optical fields, as well as chirping effects. Based on this distributed model, the cascaded TWEAM structure demonstrates optical pulses of less than 4-ps width at a 40-GHz repetition rate, while maintaining high-optical output powers and extinction ratios. Additionally, the phase-matching capability of the cascade structure, in comparison to single device operation, allows for a higher tolerance of TWEAM design against distributed effects.

#### REFERENCES

- [1] S. Kawanishi, Y. Miyamoto, H. Takara, M. Yoneyama, K. Uchiyama, I. Shake, and Y. Yamabayashi, "120 Gbit/s OTDM system prototype," in *ECOC '98 Tech. Dig.*, pp. 43–45.
- [2] B. Mikkelsen, G. Raybon, R.-J. Essiambre, K. Dreyer, Y. Su, L. E. Nelson, J. E. Johnson, G. Shtengel, A. Bond, D. G. Moodie, and A. D. Ellis, "160 Gbit/s single-channel transmission over 300 km nonzero-dispersion fiber with semiconductor based transmitter and demultiplexer," in *ECOC '99*, 1999, Postdeadline Paper D2-3.
- [3] V. Kaman and J. E. Bowers, "120 Gbit/s OTDM system using electroabsorption transmitter and demultiplexer operating at 30 GHz," *Electron. Lett.*, vol. 36, pp. 1477–1479, 2000.
- [4] S. Z. Zhang, Y. J. Chiu, P. Abraham, and J. E. Bowers, "25 GHz polarization-insensitive electroabsorption modulators with traveling-wave electrodes," *IEEE Photon. Technol. Lett.*, vol. 11, pp. 191–193, Feb. 1999.
- [5] V. Kaman, Y. J. Chiu, T. Liljeberg, S. Z. Zhang, and J. E. Bowers, "Integrated tandem traveling-wave electroabsorption modulators for >100 Gbit/s OTDM applications," *IEEE Photon. Technol. Lett.*, vol. 12, pp. 1471–1473, Nov. 2000.
- [6] D. D. Marcenac, A. D. Ellis, and D. G. Moodie, "80 Gbit/s OTDM using electroabsorption modulators," *Electron. Lett.*, vol. 34, pp. 101–103, 1998.
- [7] G. L. Li, C. K. Sun, S. A. Pappert, W. X. Chen, and P. K. L. Yu, "Ultrahigh-speed traveling-wave electroabsorption modulator-design and analysis," *IEEE Trans. Microwave Theory Technol.*, vol. 47, pp. 1177–1183, July 1999.
- [8] G. P. Agrawal, *Nonlinear Fiber Optics*. New York: Academic, 1995.
- [9] K. S. Giboney, M. J. W. Rodwell, and J. E. Bowers, "Traveling-wave photodetector design and measurements," *IEEE J. Select. Topics Quantum Electron.*, vol. 2, pp. 622–629, Sept. 1996.
- [10] R. E. Collin, *Foundations for Microwave Engineering*. New York: McGraw-Hill, 1966.
- [11] F. Devaux, Y. Sorel, and J. F. Kerdiles, "Simple measurement of fiber dispersion and of chirp parameter of intensity modulated light emitter," *J. Lightwave Technol.*, vol. 11, pp. 1937–1940, Dec. 1993.